ANTIMICROBIAL AGENTS AND CHEMOTHERAPY, Mar. 2011, p. 1296–1299 Vol. 55, No. 3
0066-4804/11/$12.00 doi:10.1128/AAC.00948-10


# Therapeutic Efficacy of Halocidin-Derived Peptide HG1 in a Mouse Model of Surgical Wound Infection with Methicillin-Resistant *Staphylococcus aureus*▽

Young Shin Lee,[1] Yong Pyo Shin,[1] Seo Hwa Shin,[1] Seungmi Park,[2] Myung Hwa Kim,[3] and In Hee Lee[1]*

*Department of Biotechnology[1] and Nursing,[2] Hoseo University, Asan City, Chungnam, South Korea, and Department of Dermatology, College of Medicine, Dankook University, Cheonan, Chungnam 330-714, South Korea[3]*

Received 13 July 2010/Returned for modification 9 November 2010/Accepted 25 December 2010

**We evaluated the therapeutic potential of HG1, an antimicrobial peptide, as a novel topical antibiotic by the use of a mouse surgical wound model of infection with methicillin-resistant *Staphylococcus aureus*. First, we attempted to determine whether or not HG1 infiltrated into the dermis when topically administered. Second, we evaluated the antibiotic effects of HG1 on skin infection via bacterial-enumeration and microscopic analyses. The results showed that topically administered HG1 was capable of penetrating into the dermis at the infection site, where it exerted its antimicrobial effects.**

As has been asserted in many clinical infection management studies, rapidly emerging antibiotic-resistant microbes pose a serious threat to the treatment of skin and soft tissue infections. Over the past 2 decades, the cationic antimicrobial peptide (AMP) has been regarded as a promising candidate for use as a novel antibiotic capable of coping with a broad variety of recalcitrant pathogens. In evaluations of this antibiotic as an alternative to existing therapeutic options for the topical treatment of superficial infections, it has been well established that AMPs have several advantages over conventional antibiotics, including a broad antimicrobial spectrum, a distinct mode of action, and rapid microbicidal time (8, 9). HG1 is a synthetic peptide derived from a natural AMP (halocidin) detected in the hemocytes of a tunicate, *Halocynthia aurantium* (3, 4, 5). Figure 1 shows the primary structures of halocidin and HG1. Previously, it was determined that HG1 retained several favorable antimicrobial features that might be commensurate with those of an effective antibiotic drug (3, 10). In particular, it was recently demonstrated that the antimicrobial activity of HG1 was resistant to proteolytic attacks by a variety of proteases generated from the human skin and pathogens (10), thus bolstering its therapeutic benefits for topical administration onto skin and soft tissue infection sites. We are currently attempting to develop HG1 into a new antibiotic for the treatment of superficial infections induced by microbes resistant to conventional drugs. In this study, the transdermal permeativity and therapeutic effects of HG1 were assessed in a mouse model of skin infection, in order to evaluate the pharmaceutical potential of HG1 as a novel topical antibiotic.

All animal experiments were conducted in accordance with the recommendations found in the Guide for the Care and Use of Laboratory Animals published by the National Institutes of Health and were approved by the Institutional Animal Care and Use Committee of Hoseo University, South Korea. Seven- to 8-week-old female ICR mice (DBL, Chungbuk, South Korea) were used in all experiments. The mice were anesthetized via intramuscular injections of Zoletil 50 (Virbac, France) at a dosage of 50 mg/kg of body weight. In order to assess the skin permeability of HG1, the shaved back skin of each experimental mouse was scratched with No. 600 sandpaper (Deerfos, Incheon, South Korea). A plastic cylinder with a diameter of 1.65 cm was affixed to the abrasion site using cyanoacrylate adhesive (Fig. 2A). A 200-μl volume of 1% (wt/vol) HG1 solution (10 mM sodium phosphate [NaP] buffer [pH 7.4] [10%], polyethylene glycol 400 [45%], glycerol [45%]) was poured into the cylinder chamber. The cylinder was removed at a predetermined time, after which the skin was washed extensively with NaP buffer (pH 7.4) to completely remove any HG1 that might remain on the surface of the skin. An area of skin (1-by-1 cm) was then excised and laid out on a slide glass. The skin samples were then frozen at −80°C for 1 h. A constant volume of tissue was obtained from each of the frozen skin samples by the use of a biopsy punch with a diameter of 8 mm. The isolated tissues were homogenized in liquid nitrogen, and the proteins were extracted from the homogenates via overnight shaking in 0.5 ml of 5% acetic acid. After brief centrifugation, 0.1 ml of the supernatant was subjected to C18 reversed-phase high-performance liquid chromatography (HPLC) and immunoblotting analysis. As shown in the HPLC profiles of Fig. 2B, the quantities of HG1 detected increased with elapsing time after HG1 treatment (Fig. 2B, upper panels). Additionally, the results of immunoblotting analysis conducted with anti-HG1 antibody (Ab) were consistent with the results of HPLC analysis (Fig. 2C). Alternatively, the skin sample (1-by-1 cm) was directly fixed for 12 h in 4% paraformaldehyde. It was then processed and embedded in paraffin, and 5-μm-thick sections were prepared. The slides were then stained with rabbit anti-HG1 Ab and the secondary Ab (anti-rabbit IgG Ab) labeled with Alexa Fluor 488 (Invitrogen) and observed under fluorescence microscopy (Fig. 2B, lower pan-

* Corresponding author. Mailing address: Department of Biotechnology, Hoseo University, 165 Sechuli, Baebang, Asan City, Chungnam 336-795, South Korea. Phone: 82-41-540-5626. Fax: 82-41-548-6231. E-mail: leeih@hoseo.edu.

▽ Published ahead of print on 10 January 2011.


FIG. 1. The primary structure of halocidin and HG1. Vertical bars in the sequence signify a disulfide bond between two cysteine residues. Asterisks indicate C-terminal amidation.

els). As can be seen in the fluorescence images shown in Fig. 2B, it was determined that HG1 infiltrated more deeply into the skin with progressing treatment time. Collectively, our results demonstrated that HG1 administered to the surface of mouse skin could penetrate into the dermis without degradation, as the integrity of the peptide was confirmed via HPLC and immunoblotting analyses. Indeed, the structural stability of HG1 infiltrated into the mouse skin was expected on the basis of the findings of the previous study, which demonstrated the resistance of HG1 to proteases occurring in human wound fluid (10).

The mouse surgical wound infection model was established as previously described (6), with some modifications. In brief, sterile silk sutures (surgical suture no. 3; Won Industry, Kyounggi, South Korea) were cut into lengths of 1.8 cm and soaked for 30 min in 3-h broth cultures of log-phase methicillin-resistant *Staphylococcus aureus* (MRSA) ($2 \times 10^9$/ml) that had been clinically isolated from a human skin infection. For reference, according to the methods recommended by the Clinical and Laboratory Standards Institute (1), it was previously determined that the MIC of HG1 for the MRSA strain used in this study is 4 μg/ml. The sutures were removed, dried on sterile filter paper, and then stored at 4°C until use. The fur on the mouse's back was clipped, and the skin was swabbed with polyvinylpyrrolidone (Povidone)-iodine (Green Pharmaceutical Co., Chungbuk, South Korea) and 70% ethanol. To insert the inoculated suture under the skin, a full-thickness incision approximately 1.5 cm in length was made. After suture insertion, the wound was secured by knotting. As shown in Fig. 3A, one end of the inserted suture was arranged in a manner that ensured that it was always available for visual inspection on the wound site. The wound was subsequently covered with DuoDERM-Extra Thin dressing (ConvaTec, Princeton), and the mice were allowed to recover. One wound was created per animal. Treatment was initiated at 2 days after surgery. First, the inserted suture was removed from the wound site using forceps, and 20 μl of 5% (wt/vol) HG1 solution was applied to the surface of the wound and spread over the area. Next, the solution was applied a second time 12 h later, and therapy was continued twice daily for a period of 5 days. A vehicle solution containing no HG1 was used as a control. As indicated in Fig. 3B, four tissue biopsy specimens were obtained from the wound by the use of a biopsy punch with a diameter of 2 mm. The total weight of the four isolated biopsy specimens was approximately 8 mg. The tissue biopsy specimens were then placed in 400 μl of Hanks' balanced salt solution (HBSS) and homogenized in a tissue grinder. The tissue homogenate was serially diluted 10-fold and plated on tryptic soy agar (TSA;

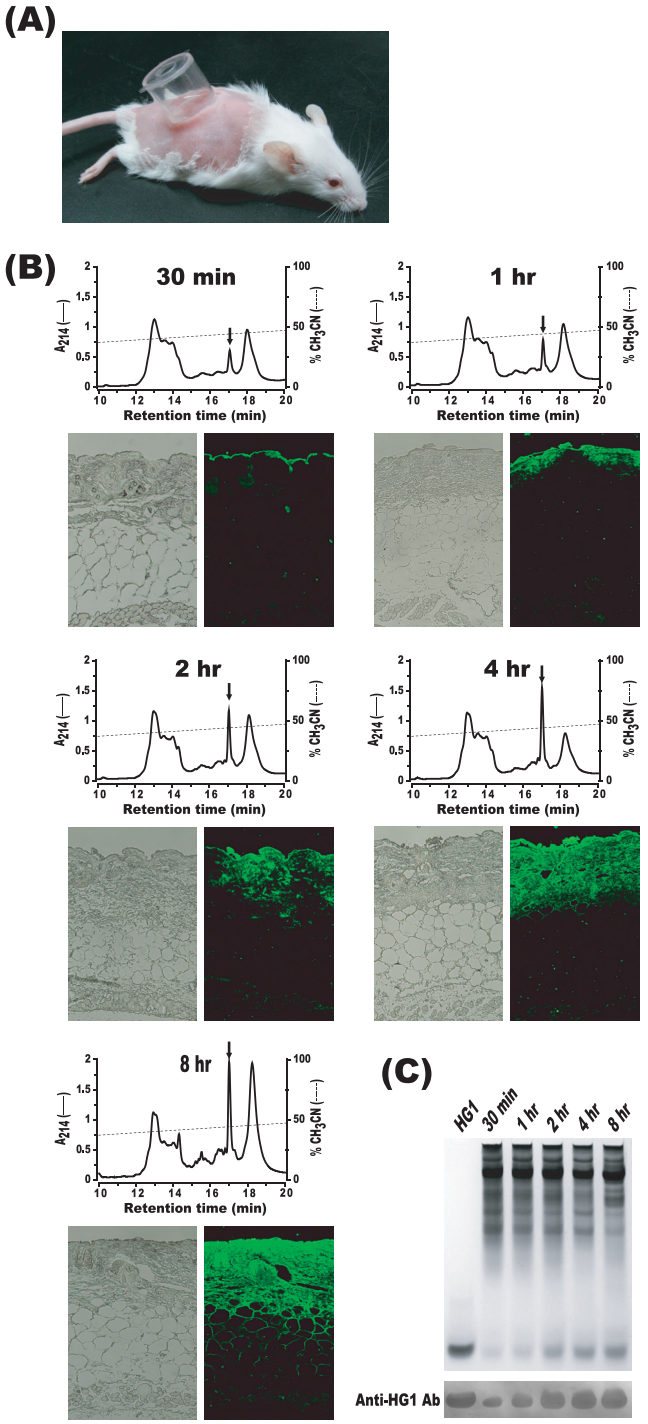


FIG. 2. Permeation of HG1 into the mouse skin. (A) HG1 was administered into an open plastic cylinder that was affixed to the skin with adhesive. (B) Each skin sample was removed from the mice at a predetermined time after the topical administration of HG1. The skin biopsy specimens were used for HPLC or immunohistochemical analyses. On the fluorescence microscopic images, HG1 appeared green because it was stained with anti-HG1 Ab and the secondary Ab labeled with Alexa Fluor 488. In each of reversed-phase HPLC profiles, the arrow indicates an HG1 peak eluted from the HPLC column. (C) Constant volumes of protein samples extracted from the skin were subjected to acid urea-polyacrylamide gel electrophoresis and immunoblotting analysis. The gels were stained with Coomassie blue.

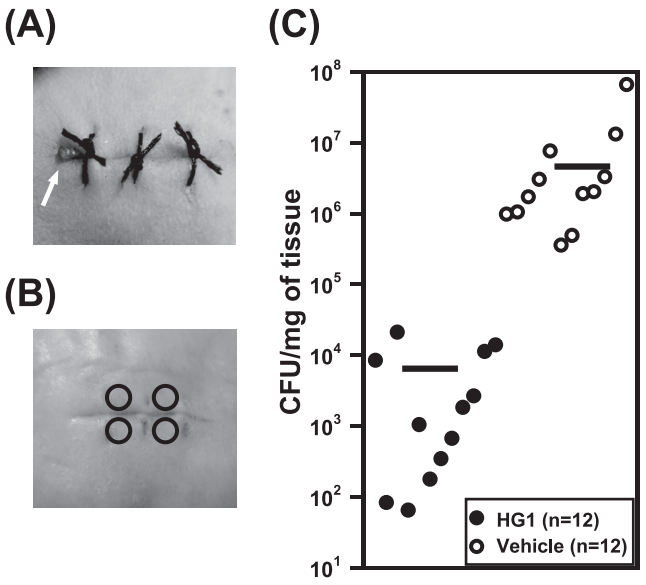


FIG. 3. Therapeutic effect of HG1 on MRSA-infected ICR mice. (A) A full-thickness wound was created on the dorsal side of the mouse and infected via insertion of a white silk suture contaminated with MRSA; the wound was stitched up with black silk sutures. An arrow indicates the white silk suture exposed on the wound surface. (B) Skin biopsy specimens were obtained from the skin using a biopsy punch. Four circles indicate the punched-out sites. (C) Numbers of recovered MRSA were expressed in terms of CFU counts per milligram of tissue. All results are separately indicated. The mean value of the data for each group is shown as a horizontal bar.

Difco) broth. After overnight culture at 37°C, the numbers of recovered CFU of MRSA were counted and converted to values representing CFU counts per milligram of tissue. As shown in Fig. 3C, the skin biopsy specimens of HG1-treated mice ($n = 12$) were found to have significantly reduced CFU counts relative to the vehicle control samples ($n = 12$). The mean CFU of MRSA recovered from the wounds treated with HG1 was almost 3 $\log_{10}$ lower than that of the MRSA recovered from the vehicle-treated wounds.

For the *in situ* detection of MRSA in the mouse skin after infection, we utilized MRSA labeled with ethidium bromide (EtBr). The 3-h broth culture of log-phase MRSA was resuspended in Dulbecco's phosphate-buffered saline (DPBS; pH 7.2) ($2 \times 10^9$/ml) and washed three times in DPBS. The bacterial suspension was then mixed with EtBr solution to achieve a final concentration of 1.25 μg/ml and incubated for 30 min at 37°C in darkness. The MRSA mixture was washed 10 times with DPBS to remove excess EtBr and then resuspended in 1 ml of DPBS. In these experiments, the skin wound infection was established without using sutures inoculated with MRSA. A full-thickness incision was made by the previously described procedure. A 10-μl volume of EtBr-labeled MRSA was inoculated into the wound site and secured by knotting, and the wound site was then covered with DuoDERM-Extra Thin dressing. At 12 h after surgery, 20 μl of 5% (wt/vol) HG1 solution was applied to the wound and spread over the area. At 4 h after the topical administration of HG1, the skin tissue (1-by-1 cm) was isolated and processed for confocal microscopic analysis according to the procedure described above.

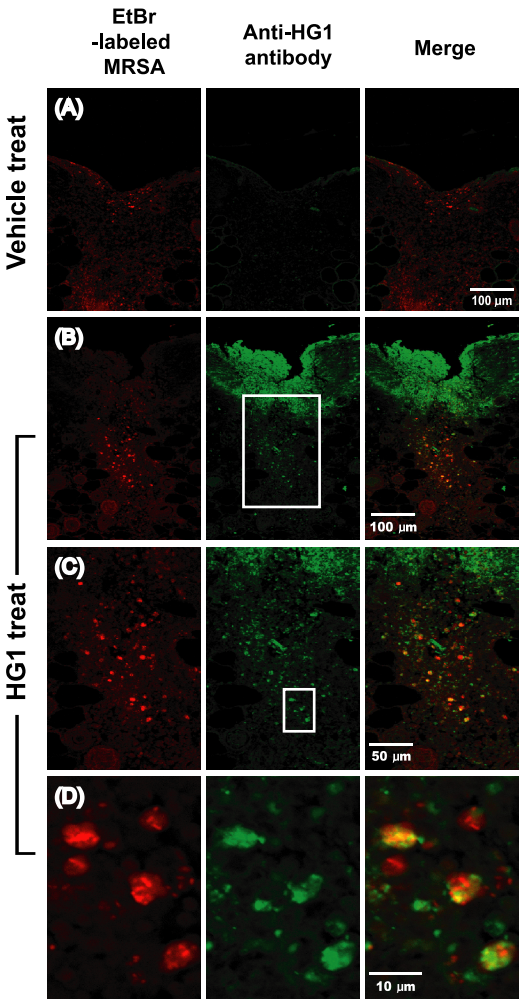


FIG. 4. Confocal microscopic observation of skins obtained from MRSA-infected mice treated with HG1 or vehicle. HG1 appear green, as it was stained with anti-HG1 Ab and the secondary Ab labeled with Alexa Fluor 488, and bacteria appear red from EtBr labeling. (A) Fluorescence image of the skin from a vehicle-treated mouse. (B) Fluorescence image of the skin from an HG1-treated mouse. (C) Enlarged image of indicated region of panel B. (D) Enlarged image of indicated region of panel C. In merged images of panels B, C, and D, the majority of the bacteria appeared to be overlapped with HG1, resulting in a yellow-orange shade.

The confocal sections were visualized separately under two different fluorescence channels; light green and red spots represented HG1 and MRSA, respectively (Fig. 4). The two images were then merged to visualize the antibiotic efficacy of HG1 against bacteria that had infected the skin. In the merged images, we could see that many of the MRSA colonies shown in red overlapped the HG1 peptide shown in green and thus appeared yellow-orange. Therefore, it was concluded that HG1 administered onto the skin wound had infiltrated successfully into the dermal infection site and also successfully bound to MRSA, thus enabling it to exert its antimicrobial effects. For the confocal microscopic observation, sequential optical sections were visualized under an FV500 laser-scanning confocal microscope (Olympus); only one section is shown.

Two major considerations must be taken into account when

employing cationic antimicrobial peptides as a topical antibiotic: the efficacy of transdermal delivery upon topical application and the presence of sufficient structural stability to ensure that the peptide persists long enough to exert its effects in the infection site (2, 7). In this report, we have endeavored to show that HG1 is a convincing candidate for a novel topical antibiotic and that it possesses the two essential features described above. As a consequence, we were able to confirm the successful infiltration of HG1 into the dermis while it maintained its structural stability (Fig. 2), and we also observed that it exerted its characteristic antimicrobial effects against MRSA bacteria present in the skin wound infection site (Fig. 4). Additionally, the therapeutic efficacy of HG1 as a topical antibiotic was confirmed via bacterial-enumeration experiments (Fig. 3). We believe that this study may represent significant progress toward a broader objective—specifically, the invention of a novel peptide antibiotic useful for the treatment of a number of pathogenic microbes that are resistant to currently available drugs.

This work was supported by a grant from the World-Class 2030 Project of Hoseo University.

## REFERENCES

1. **Clinical and Laboratory Standards Institute.** 2006. Methods for dilution antimicrobial susceptibility tests for bacteria that grow aerobically, 7th ed. Approved standard M7-A7. Clinical and Laboratory Standards Institute, Wayne, PA.
2. **Hancock, R. E., and H. G. Sahl.** 2006. Antimicrobial and host-defense peptides as new anti-infective therapeutic strategies. Nat. Biotechnol. **24:**1551–1557.
3. **Jang, W. S., et al.** 2003. Biological activities of synthetic analogs of halocidin, an antimicrobial peptide from the tunicate *Halocynthia aurantium*. Antimicrob. Agents Chemother. **47:**2481–2486.
4. **Jang, W. S., et al.** 2006. Antifungal activity of synthetic peptide derived from halocidin, antimicrobial peptide from the tunicate, *Halocynthia aurantium*. FEBS Lett. **580:**1490–1496.
5. **Jang, W. S., K. N. Kim, Y. S. Lee, M. H. Nam, and I. H. Lee.** 2002. Halocidin: a new antimicrobial peptide from hemocytes of the solitary tunicate, *Halocynthia aurantium*. FEBS Lett. **521:**81–86.
6. **McRipley, R. J., and R. R. Whitney.** 1976. Characterization and quantitation of experimental surgical wound infections used to evaluate topical antibacterial agents. Antimicrob. Agents Chemother. **10:**38–44.
7. **Oyston, P. C., M. A. Fox, S. J. Richards, and G. C. Clark.** 2009. Novel peptide therapeutics for treatment of infections. J. Med. Microbiol. **58:**977–987.
8. **Reddy, K. V., R. D. Yedery, and C. Aranha.** 2004. Antimicrobial peptides: premises and promises. Int. J. Antimicrob. Agents **24:**536–547.
9. **Shai, Y.** 2002. Mode of action of membrane active antimicrobial peptides. Biopolymers **66:**236–248.
10. **Shin, Y. P., et al.** 2010. Antimicrobial activity of a halocidin-derived peptide resistant to attacks by proteases. Antimicrob. Agents Chemother. **54:**2855–2866.